Journal of Petroleum Science and Engineering 208 (2022) 109450

Contents lists available at ScienceDirect

Journal of Petroleum Science and Engineering

journal homepage: www.elsevier.com/locate/petrol

Subsea field layout optimization (Part I) – directional well trajectory planning based on 3D Dubins Curve

Haoge Liu [a,*], Tor Berge Gjersvik [a], Audun Faanes [a,b]

[a] Department of Geoscience and Petroleum, Norwegian University of Science and Technology, Norway
[b] Equinor ASA, Norway

ARTICLE INFO

Keywords:
Well trajectory
Well profile
Well path
3D dubins curve
Optimization

ABSTRACT

Directional well trajectory planning, which includes the optimization of the drilling site location and the trajectory between the drilling site to the completion interval, plays an important role in reducing subsea field development cost. The traditional well trajectory planning methods are based on the projected 2D profile of the wellbore trajectory with empirical knowledge or trial-and-error method to select a proper drilling site. In this study, we propose a new efficient optimization method based on the 3D Dubins curve, which has been widely used in autopilot for path planning but has never been mentioned in drilling industry. In short, we use gradient descent method to find the best drilling site location while adopting the 3D Dubins curve as the optimal wellbore trajectory to reach each completion interval so that the "1-site-*n*-wells" problem can be easily solved. Abundant case studies including both mathematically representative cases and the real practical field cases are conducted to demonstrate the feasibility and efficiency of our method. Wider application of our method for more complex situations are also discussed. This work is the first of a series of papers which systematically introduce an efficient method for subsea field layout optimization to minimize the development cost.

1. Introduction

Industry benchmarks show a significant increase in oil and gas field development cost over last decade. The cost challenge is much harsher in subsea field development. According to the report (Skaugset, 2015) released by Norway's Oil and Gas Technology Strategy for 21st Century (OG21), the subsea cost tripled from the year 2005–2013. Taking the low oil price and its volatility into account, it's crucial to cut the subsea development cost to maintain the industry profitability.

Subsea development involves quite a complicated procedure where the layout design plays one of the most important roles to cut the overall cost. From the reservoir to the topside facility, the layout design mainly includes well trajectories, positions of drilling sites and manifolds, flowline and cable routing, etc. In order to achieve the overall minimum cost, we need not only a method to achieve the optimum in every single designing phase, but also to find the interrelationships of cost within all these phases. In this study, we propose a method for directional well trajectory planning so that we can find out the optimal position of one drilling site to reach a given set of completion intervals with optimal trajectories.

Directional well trajectory planning is one of the most difficult tasks in field development because of too many different types of constraints and the unpredictable incurring cost. Statistically, the well drilling cost is almost linearly related with the trajectory length. The work of D. S. Amorim Jr (Amorim et al., 2019). reveals that the cost per meter always converges to a stable value as the well length increases, proving the statistically linear relationship between the drilling cost and the wellbore length. Based on the statistical result, the optimal trajectory can be considered as the shortest trajectory with curvature constraints. Even though, practically, the shortest trajectory may not be the optimal because of the complex downhole situations, it's still the design basis for well planning.

The curvature constrained method for well trajectory optimization dates back to the early 1970s (Taylor and Mason, 1972; Zaremba, 1973) when directional drilling technology started to be developed. Since then, it has evolved several types of curves (McMillian, 1981; Shengzong et al., 1999; Sawaryn and Thorogood, 2005; Samuel, 2010; Ilyasov et al., 2014; Liu and Samuel, 2014; Yi and Samuel, 2015; Mittal and Samuel, 2016; Wang et al., 2019) for the well trajectory, including the circular arc, the polynomial spline, the catenary and the clothoid or the Euler spiral. However, all these decades, the drilling industry seemed to overlook the Dubins curve (Dubins, 1957) which exactly gives the

* Corresponding author.
E-mail address: haoge.liu@ntnu.no (H. Liu).

https://doi.org/10.1016/j.petrol.2021.109450
Received 30 October 2020; Received in revised form 17 August 2021; Accepted 1 September 2021
Available online 4 September 2021

shortest curvature-constrained path between two directional points in 2D given that the moving direction is only forward.

Dubins concluded that the shortest path is made by joining circular arcs of maximum curvature and a straight line, which was later proved by Johnson (Johnson, 1974) by using Pontryagin's maximum principle. In details, the Dubins curve is comprised of two families which are the CCC and CSC, where "C" stands for circular arc, and "S" stands for straight line. The CCC family consists of RLR and LRL, where "R" stands for right turn, and "L" stands for left turn. The CSC family consist of RSR, RSL, LSR, LSL. The shortest path is one of the six patterns, as shown in Fig. 1. While extending the original 2D Dubins curve into 3D, Sussman (Sussmann, 1995) pointed out a situation when the two points are too close, the optimal path should be helicoidal which can be regarded as a special CCC pattern. Till now, the Dubins curve has already matured in the autopilot industry for path planning of cars, robots, UAVs, AUVs, etc (Chitsaz and Lavalle, 2008; Patsko and Turova, 2009; Hota and Ghose, 2010; Owen et al., 2015; Pharpatara et al., 2015; Wang, 2018).

The drilling process is almost the same as the piloting process, and the well trajectory planning is essentially a path planning. Obviously, CCC family is not suitable for drilling because of the large turning angle in the trajectory. Hence, here in this study, we will extend the CSC patterns of the original 2D Dubins curves into 3D as the optimal well trajectory for well planning. The property of Dubins curve not only guarantees the shortest path but also minimizes the length of curved section. Consequently, the straight section of Dubins curve avoids higher inclination angles than necessary. All these features are beneficial for drilling.

By adopting the Dubins curve for the optimal wellbore trajectory, we can then use gradient descent method to determine the optimal drilling site for a cluster of wells or to design a multilateral well to reach several completion intervals. In the following content, we will show the feasibility and efficiency of our well trajectory planning method which combines the Dubins curve strategy and the gradient descent method in solving the "1-site-*n*-wells" problem. Wider application of our method will also be discussed after case studies.

2. Problem description and basic assumptions

2.1. Problem description

Given k well completion intervals, $k \in Integer^{+}$, each completion interval is defined by its start point $P_{2,i} = (Px_{2,i}, Py_{2,i}, Pz_{2,i})$ and the drilling direction vector $V_{2,i} = (Vx_{2,i}, Vy_{2,i}, Vz_{2,i})$ where $Vz_{2,i} \leq 0$ to ensure the direction is not upward; the highest allowed kickoff point $P_{1,i} = (Px_1, Py_1, Pz_{1,i})$ for every wellbore should be at the depth of Z_i m, i.e. $Pz_{1,i} = Z_i < 0$, $i \in \{1, 2, \ldots, k\}$. The drilling direction vector at every kickoff point is vertical downwards $V_{1,i} = (0, 0, -1)$. The

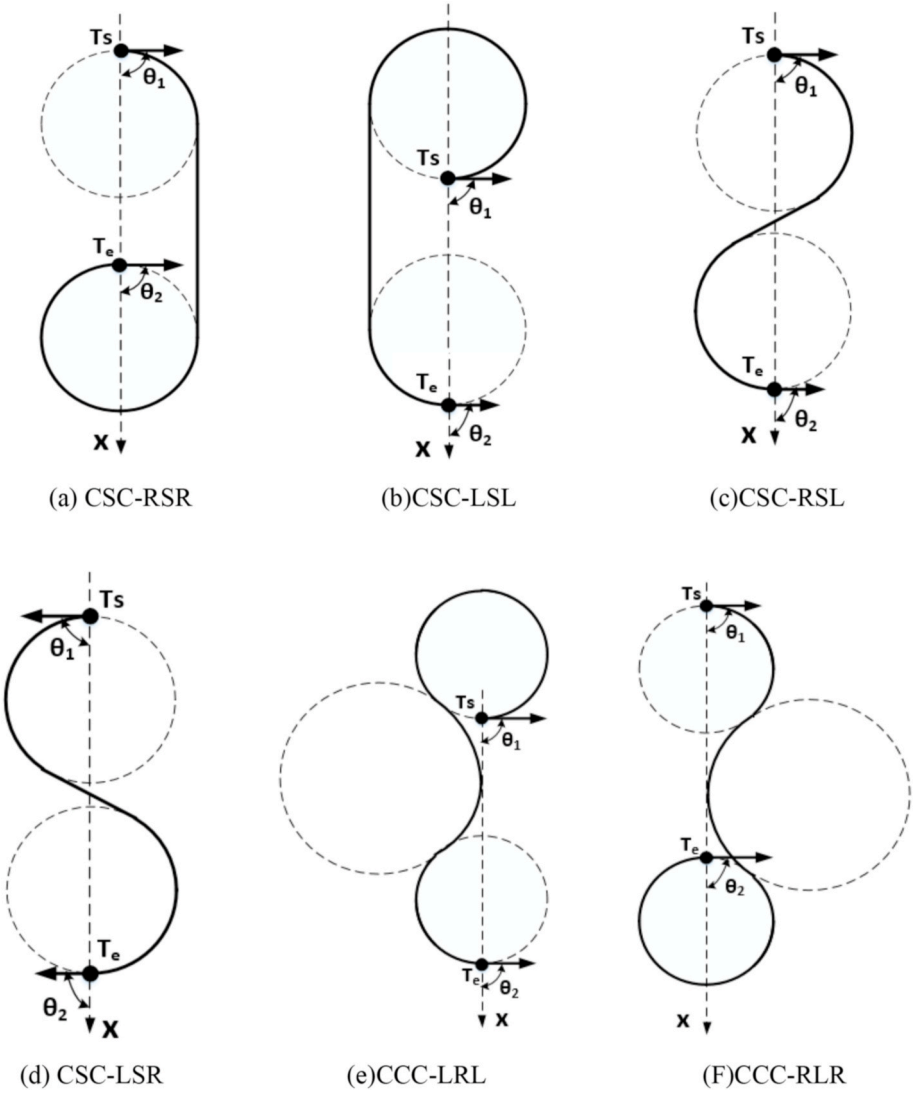

Fig. 1. Patterns of 2D Dubins Curve (modified based on (Wang, 2018)).

maximum allowed turning rate/dogleg severity is $\kappa°/30$ m, i.e. minimum allowed turning rate radius is $r_{\min} = \frac{5400}{\pi\kappa}$m. The cost of a wellbore trajectory can be a user-defined function related with the trajectory structure following the form as $COST = cstC(Lc) + cstS(Ls,\theta)$, where Lc is the length of non-straight section, Ls is the length of straight section, θ is the deviation angle of the straight section; $cstC(Lc)$ is the cost function of non-straight section which is continuous and positively correlated with Lc, i.e. $\frac{\partial\, cstC(Lc)}{\partial\, Lc} > 0$; $cstS(Ls,\theta)$ is the cost function of straight section which is continuous and positively correlated with Lc and θ, i.e. $\frac{\partial\, cstS(Ls,\theta)}{\partial\, Ls} > 0$ and $\frac{\partial\, cstS(Ls,\theta)}{\partial\, \theta} > 0$.

The objective is to find the optimal drilling site $D:(Px_1, Py_1, 0)$ to drill multiple wells from one drill site such that they can reach all completion intervals with the total cost of all trajectories minimized while fulfilling the dogleg severity constraint. We can simply call this "1-site-*n*-wells" problem.

2.2. Basic assumption and simplification

1. The formation underground is drillable in all directions.
2. The surface for the drilling site is a horizontal plane $z = 0$.
3. Every completion interval is reasonable, so that it is easily reachable. For example, if the maximum allowed turning rate/dogleg severity is $1.5°/30$ m, i.e. the minimum curvature radius is $r = 1145.9$ m, while the start point of the completion interval is too shallow at $Pz_2 = -1000$ m, and the vector is required to be horizontal $V_2 = (-1, 0, 0)$, then such a completion interval is considered as unreasonable, because we cannot reach such a completion interval with an easy trajectory as we have to drill below the interval depth and then drill upwards even if the wellbore starts to kick off at the surface, unless we reduce the turning rate radius, i.e. increase the dogleg severity. As shown in Fig. 2.
4. For wells drilled from one drilling site, the difference within the exact locations of wellheads is quite small, hence we can consider all wellheads' locations are the same as the drilling site location.

3. Methodology

3.1. Mathematical model and brief analysis

This optimization problem can be divided into two levels. The first level is to find the optimal trajectory of minimum cost when the completion interval (P_2, V_2) and highest allowed kickoff point (P_1, V_1) are both given:

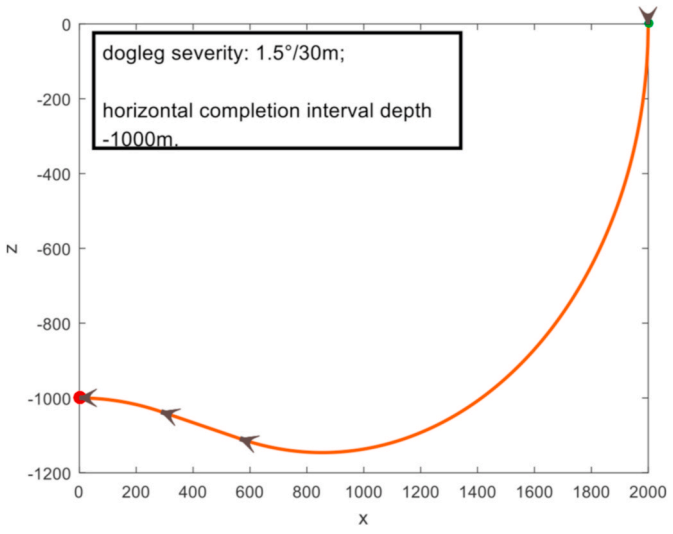

Fig. 2. Unreasonable well completion interval for a given dogleg severity.

$$\begin{aligned} &Obj. \quad \min[COST(P_1, V_1, P_2, V_2, r)] \\ &\quad = \min[cstC(Lc) + cstS(Ls, \theta)] \\ &s.t. \quad r \geq r_{\min} \end{aligned} \tag{1}$$

Equation (1) cannot implicitly tell which parameters should be taken as the variables to be optimized to achieve the objective. Given $\frac{\partial\, cstC(Lc)}{\partial\, Lc} > 0$, $\frac{\partial\, cstS(Ls,\theta)}{\partial\, Ls} > 0$ and $\frac{\partial\, cstS(Ls,\theta)}{\partial\, \theta} > 0$, the objective can be converted into Equation (2) if Lc, Ls and θ can reach minimum at the same time with the r constraint. It should be noted that Lc, Ls and θ are function of (P_1, V_1, P_2, V_2, r), for convenience, we just write as Lc, Ls and θ rather than $Lc(P_1, V_1, P_2, V_2, r)$, $Ls(P_1, V_1, P_2, V_2, r)$ and $\theta(P_1, V_1, P_2, V_2, r)$.

$$\begin{aligned} &Obj. \quad \min[cstC(Lc) + cstS(Ls, \theta)] \\ &\quad = cstC(\min(Lc)) + cstS(\min(Ls), \min(\theta)) \\ &s.t. \quad r \geq r_{\min} \end{aligned} \tag{2}$$

The Dubins curve which starts from the highest allowed kickoff point to the start point of completion interval just fulfills Equation (2). Practically, the curved wellbore section is more costly than the straight section, i.e. $\frac{\partial\, cstC(Lc)}{\partial\, Lc} > \frac{\partial\, cstS(Ls,\theta)}{\partial\, Ls}$, hence minimizing the curved length is prior compared to minimizing the straight length in cutting the overall cost. While ensuring the curved length L_c to be minimum, the Dubins curve also minimizes the total length of the curve $L_c + L_s$ between two directional points, i.e. $L_s$is minimized as well. What's more, Dubins curve makes the straight section to be less inclined in our drilling scenario where $V_0 = [0, 0, -1]$, which means θ is also minimized. Hence the solution of the first level optimization problem is to find the Dubins curve, and Equation (1) becomes equivalent to Equation (3). Equation (3) is just to find out the Dubins curve given (P_1, V_1, P_2, V_2, r). In section 3.2, we will see that finding the Dubins curve is solving a set of three transcendental equations.

$$\begin{aligned} &Obj. \quad \min[COST(P_1, V_1, P_2, V_2, r)] \\ &\quad = cstC(Lc) + cstS(Ls, \theta) \\ &s.t. \quad r \geq r_{\min} \\ &\quad Lc, Ls, \theta \in DubinsCurve \\ &\quad Pz_1 = Z \end{aligned} \tag{3}$$

The second level is to find the optimal drilling site $D:(Px_1, Py_1, 0)$ so that the total cost of all optimal lateral trajectories is minimum, given all the completion intervals ($P_{2,i}$, $V_{2,i}$), the highest allowed kickoff points' depth $Pz_{1,i} = Z_i$ and their directions $V_{1,i}$. Compared with the first level problem, the x and y components of highest allowed kickoff point (Px_1, Py_1) becomes the unknown variables that need to be optimized. As shown in Equation (4), the second level optimization is the model for solving the whole problem.

$$\begin{aligned} &Obj. \quad \min_{D:(Px_1, Py_1)} \sum_{i=1}^{k} COST(P_1, V_1, P_2, V_2, r)_i \\ &\quad = \min_{D:(Px_1, Py_1)} \sum_{i=1}^{k} [cstC(Lc)_i + cstS(Ls, \theta)_i] \\ &s.t. \quad r_i \geq r_{\min} \\ &\quad Lc_i, Ls_i, \theta_i \in DubinsCurve \\ &\quad Pz_{1,i} = Z_i \end{aligned} \tag{4}$$

For each lateral trajectory $\forall i \in \{1, 2, \ldots, k\}$, once the drilling site $D:(Px_1, Py_1, 0)$ and the highest kickoff point's depth Z_i are given, we can obtain the minimum $COST(P_1, V_1, P_2, V_2, r)_i$ from the first level optimization whose constraints also fulfill the second level optimization. Hence by gradient descent, we can optimize the unknown variables (Px_1, Py_1) to achieve the objective, i.e. to find out the optimal drilling site to minimize the total cost. By using the Matlab built-in function "fmincon", we can easily solve the model.

3.2. 3D Dubins Curve for wellbore trajectory

The original Dubins curve (Dubins, 1957) only solved the 2D scenario, for the 3D well planning scenario, we can derive it as follows.

Given the highest allowed kickoff position $P_1 : (Px_1, Py_1, Pz_1)$ and direction vector $V_1 = (0, 0, -1)$, the well completion interval $P_2 : (Px_2, Py_2, Pz_2)$ and direction vector $V_{2,i} = (Vx_{2,i}, Vy_{2,i}, Vz_{2,i})$, as shown in Fig. 3, C_1 is the end point of the first circular section, i.e. build-up section. C_2 is the start point of the second circular section which can be either the continued build-up section as shown in Fig. 3(a) or the drop-down section as shown in Fig. 3(b) and (c). In certain cases, C_1 can coincide with P_1, C_2 can coincide with P_2. Another property of Dubins curve is that the minimum allowed curvature radius value is the radius value of both circles:

$$r = r_{\min} \tag{5}$$

Denote the straight section vector, which is unknown, as

$$T = \vec{C_1C_2} = (Tx, Ty, Tz) \tag{6}$$

The unit vector of T is

$$t = \frac{T}{\|T\|} \tag{7}$$

The vector perpendicular to the first circular plane is

$$U_1 = T \times V_1 \tag{8}$$

The radius vector oriented from P_1 towards O_1 is

$$\Omega_1 = V_1 \times U_1 \tag{9}$$

The unit vector of Ω_1 is

$$\omega_1 = \frac{\Omega_1}{\|\Omega_1\|} \tag{10}$$

Hence the center of the first circle is

$$O_1 = P_1 + r \cdot \omega_1 \tag{11}$$

The radius vector oriented from C_1 towards O_1 is

$$\Phi_1 = T \times U_1 \tag{12}$$

The unit vector of Φ_1 is

$$\varphi_1 = \frac{\Phi_1}{\|\Phi_1\|} \tag{13}$$

Therefore, the point C_1 can be expressed as

$$C_1 = O_1 - r \cdot \varphi_1 \tag{14}$$

Similarly, we can get ω_2, O_2, φ_2, and then the point C_2

$$C_2 = O_2 - r \cdot \varphi_2 \tag{15}$$

Use the definition of T to get the three unknown variables (Tx, Ty, Tz):

$$T = C_2 - C_1 \tag{16}$$

Equation (16), where C_1 and C_2 are functions of T, is a set of 3 transcendental equations with 3 unknown variables (Tx, Ty, Tz). It is almost impossible to get the explicit analytical expression for (Tx, Ty, Tz) from these transcendental equations, but we can use gradient descent algorithm to obtain their values. This can be done by using the Matlab built-in function "fsolve". After $T = (Tx, Ty, Tz)$ is calculated from Equation (16), we can calculate the other geometric parameters of the 3D Dubins curve.

The turning angle on each circular plane

$$\gamma_1 = \angle P_1O_1C_1 = \arccos\left(\frac{V_1 \cdot T}{\|V_1\| \cdot \|T\|}\right) \tag{17}$$

$$\gamma_2 = \angle P_2O_2C_2 = \arccos\left(\frac{V_2 \cdot T}{\|V_2\| \cdot \|T\|}\right) \tag{18}$$

The length of each circular section:

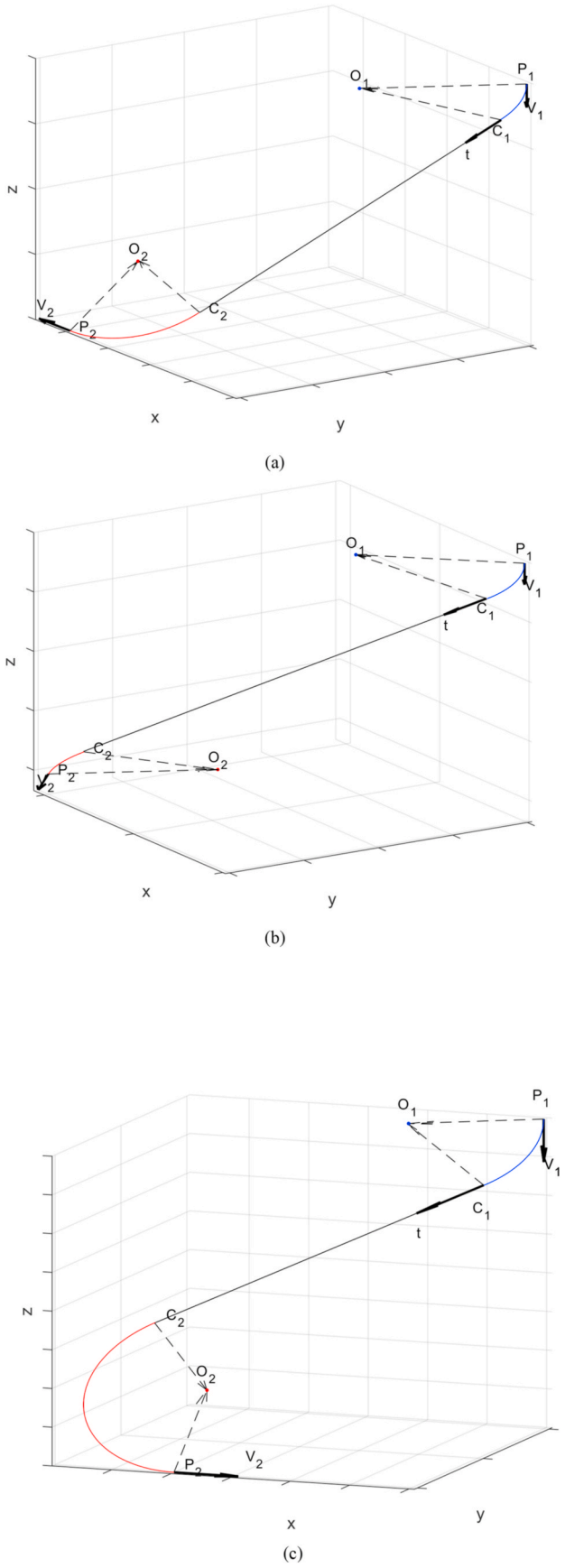

Fig. 3. 3D Dubins curve for Wellbore Trajectory.

$$L_{c1} = \gamma_1 \cdot r;\ L_{c2} = \gamma_2 \cdot r \tag{19}$$

The total curved length is the sum of two circular section:

$$Lc = L_{c1} + L_{c2} \tag{20}$$

The length of the straight section:

$$Ls = \|T\| \tag{21}$$

The calculation process not only gives us the optimal trajectory, but also tells if an assigned drilling site is suitable to drill to the completion interval. As shown in Fig. 3(c), when it requires the trajectory to turn around, i.e. γ_2 is bigger than 90°, we may consider that drilling site is not so suitable even it is feasible.

4. Case study

In this section, we first test on some special cases where the human intuition can tell the correct results to validate our method. Then we demonstrate the results for more complex general cases generated by our method. For the purpose of demonstration, assign the user-defined cost functions in a reasonable form as follows:

$$cstC(Lc) = 2Lc \tag{22}$$

$$cstS(Ls, \theta) = (1 + \sin\theta)Ls \tag{23}$$

Such cost functions indicate that the circular well trajectory is more expensive than straight trajectory because $2 \geq 1 + \sin\theta$; besides, the vertically straight well trajectory is cheaper than the inclined trajectory because $1 + \sin\theta \geq 1$, where $\theta \in \left[0, \frac{\pi}{2}\right]$. Of course, the users can assign their own cost functions as they like provided the functions are continuous and fulfill the requirements that $\frac{\partial\ cstC(Lc)}{\partial\ Lc} > 0$, $\frac{\partial\ cstS(Ls,\theta)}{\partial\ Ls} > 0$ and $\frac{\partial\ cstS(Ls,\theta)}{\partial\ \theta} > 0$.

As for the computational time, it will be trivial to report the exact time for each case, because it only takes several seconds for a case without plotting the optimal cost distribution figure, coded by Matlab, conducted on an Intel i5-4210U CPU. Such a short time on such an old CPU bespeaks the efficiency of the method, and we believe there is still space for improvement in our algorithms and codes.

4.1. Case 1: validation cases

In the validation cases, we assign representative values for the input parameters so that it's more convenient for us to have the correct intuition results and then to compare with the numerical results generated by our method. The initialization of the drilling site location for the gradient descent algorithm is set as $(1,\ 1)$ for all the following validation cases.

4.1.1. Case 1.1

For a single well completion interval, the best drilling site should be vertically above the point where the tangent vector of the circle tangential to the completion interval is straight upwards. In such a case, the optimal trajectory is essentially a 2D curve, and there is only one curved section, i.e. P_1 and C_1 coincide. As shown in Table 1 and Fig. 4. The tiny numerical error is induced by the gradient descent computation and it depends on the settings for numerical/optimality tolerance.

The optimal cost distribution of a drilling site where $Px_1, Py_1 \in [-2, 2]$ is shown in Fig. 5. The position resolution of the figure is 0.1. The blank area, as shown in Fig. 5(b), indicates that if the drilling site is located there, then the completion interval cannot be reached easily at the given turning rate constraint. In other words, a CCC family of Dubins curve is required.

From the figures we can see how the well completion interval affects the cost distribution.

Table 1
Case 1.1

Case	Input Parameters				Optimal Drilling Site (Px_1, Py_1)	
	P_2	V_2	Pz_1	$r_{\min}$	Intuition	Numerical
(a)	(0, 0, −4)	(-1, 0, 0)	−1	1	(1,0)	$(1.0000,\ -9.3944 \times 10^{-10})$
(b)	(0, 0, −3.5)	(-1, −1, 0)	−1	1	$\left(\frac{1}{\sqrt{2}}, \frac{1}{\sqrt{2}}\right)$	(0.7071, 0.7071)
(c)	(0, 0, −4)	$\left(-1,\ 0,\ -\frac{1}{\sqrt{3}}\right)$	−1	1	(0.5,0)	$(0.5000,\ -6.9746 \times 10^{-9})$

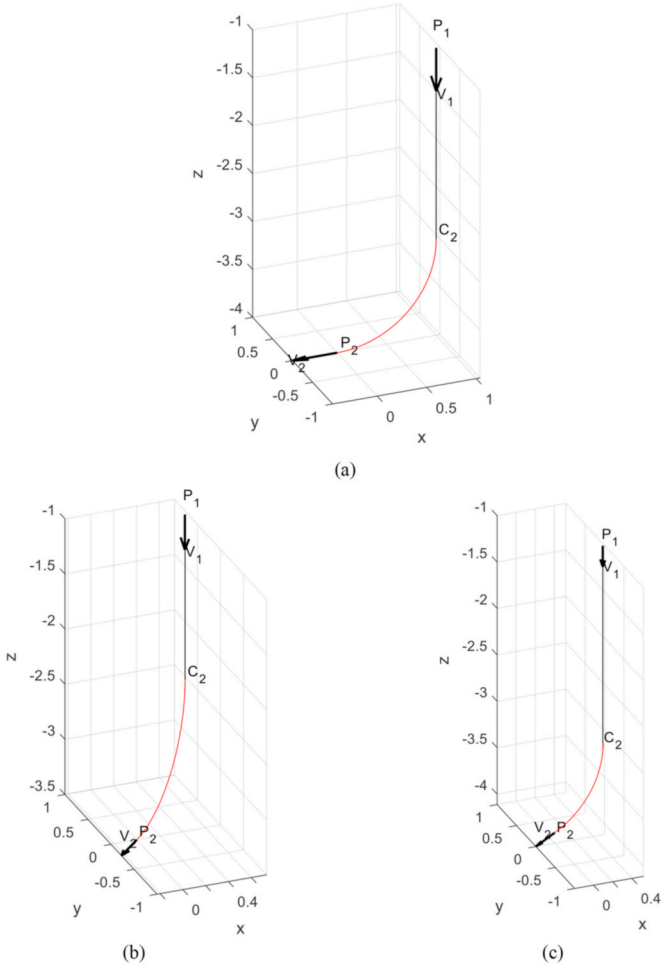

Fig. 4. Optimal drilling site and well trajectory for case 1.1.

4.1.2. Case 1.2

For an even number of well completion intervals distributed symmetrically to a vertical line, the best drilling site is the cross point of the vertical line and the surface plane. As shown in Table 2 and Fig. 6.

The optimal cost distribution of a drilling site where $Px_1, Py_1 \in [-2, 2]$ with the position resolution of 0.1 is shown in Fig. 7. From the figure, we can see the symmetrical property of the cost distribution corresponding to the symmetry of the well completion intervals. The case 1.2(a) is not just axis symmetric, but also symmetric to x-plane and y-plane, hence the cost distribution is not just an odd function, but also an even function. While the case 1.2(b) is only axis symmetric, hence the cost distribution for case 1.2(b) is just an odd function.

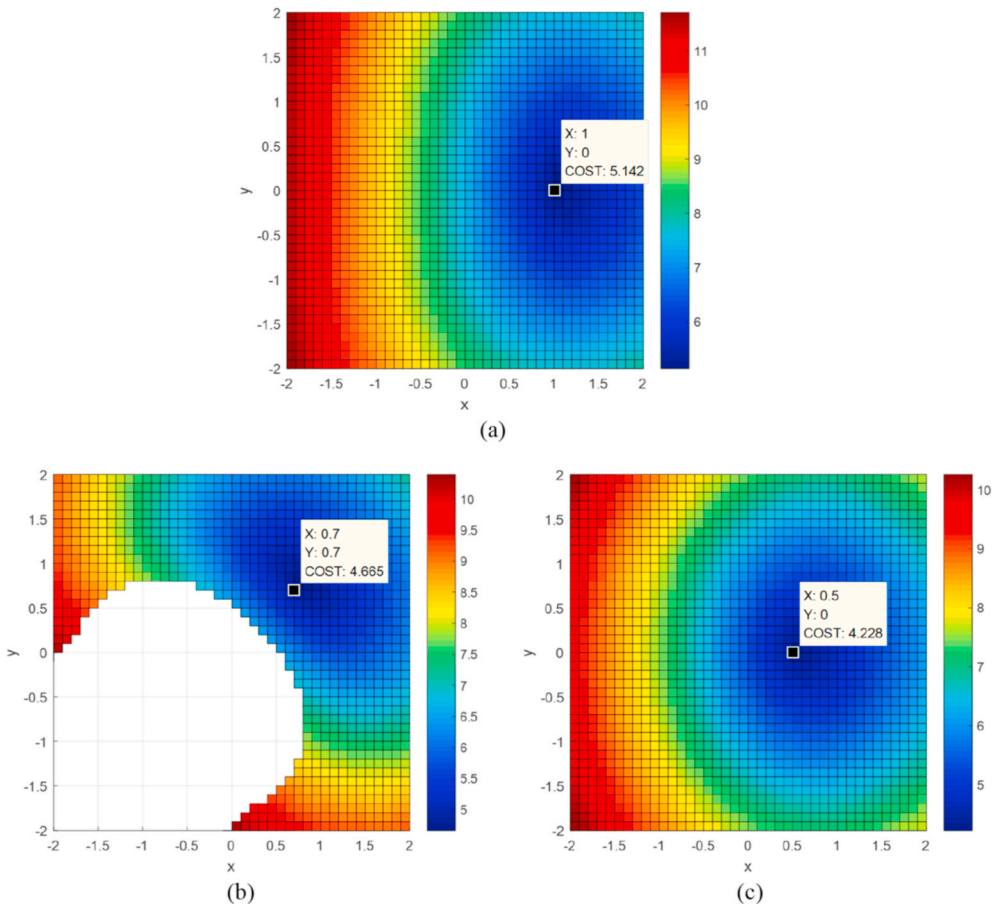

Fig. 5. Optimal cost distribution for case 1.1.

Table 2
Case 1.2

Case	Input Parameters				Optimal Drilling Site(Px_1, Py_1)	
	$P_{2,i}$	$V_{2,i}$	$Pz_{1,i}$	r_{min}	Intuition	Numerical
(a)	(2, 0, −4)	(1, 0, 0)	−1	1	(0, 0)	(0.0000, 0.0000)
	(-2, 0, −4)	(-1, 0, 0)	−1	1		
(b)	(2, 0, −4)	(1, 0, 0)	−1	1	(0, 0)	$(-1.8422 \times 10^{-17}, 3.0342 \times 10^{-16})$
	(-2, 0, −4)	(-1, 0, 0)	−1	1		
	(1.5, 1, −7)	(0, 1, 0)	−1.5	1.5		
	(-1.5, −1, −7)	(0, −1, 0)	−1.5	1.5		

4.2. Case 2: general cases

In the general cases, we use a more realistic set of completion intervals, generated by manipulating data from a real field as shown in Table 3. Highest kickoff point for all laterals is $Z_i = -300$ m.

4.2.1. Case 2.1

If the maximum allowed turning rate/dogleg severity is only 2°/30 m, i.e. minimum allowed turning rate radius is $r_{min} = 859.4$ m. The optimal drilling site and well trajectories for the 4 well completion intervals in Table 3 is shown in Fig. 8. The optimal cost distribution of a drilling site where $Px_1 \in [400, 3200]$, $Py_1 \in [200, 2100]$ with the resolution of 50 is shown in Fig. 9. The blank area indicates that if the drilling site is located there, then there is at least one completion interval that can't be reached. The data mark indicates the optimal drilling site of the lowest total cost based on the discretized values at the mesh nodes. The exact optimal drilling site location is $(Px_1, Py_1) = (1129.33, 606.19)$, and the corresponding optimal cost is 22,878.0.

4.2.2. Case 2.2

From Case 2.1, we can easily tell that it is the 4th well completion interval which is relatively shallow that causes the unreachable situation, i.e. the blank area in Fig. 9. If we don't consider the 4th well completion interval, the solution is as follows.

The optimal drilling site and well trajectories for the first 3 well completion intervals in Table 3 are shown in Fig. 10. The optimal cost distribution of a drilling site where $Px_1 \in [400, 3200]$, $Py_1 \in [200, 2100]$ with the resolution of 50 is shown in Fig. 11. The data mark indicates the optimal drilling site of the lowest total cost based on the discretized values at the mesh nodes. The exact optimal drilling site location is $(Px_1, Py_1) = (1768.28, 750.31)$, and the corresponding optimal cost is 19,367.4. As we are not considering the 4th well completion interval, there is no more blank area in Fig. 11.

4.2.3. Case 2.3

From Case 2.1, we can see that the 2nd well completion interval is not so suitable to be drilled from the same drilling site as the other 3 intervals, because it requires a big turn in the trajectory. It may be better to leave the 2nd well completion interval as a satellite well or consider it with the possible well intervals in the future development.

The optimal drilling site and well trajectories for the well completion intervals NO.1, NO.2 and NO.4 in Table 3 is shown in Fig. 12. The optimal cost distribution of a drilling site where $Px_1 \in [400, 3200]$, $Py_1 \in$

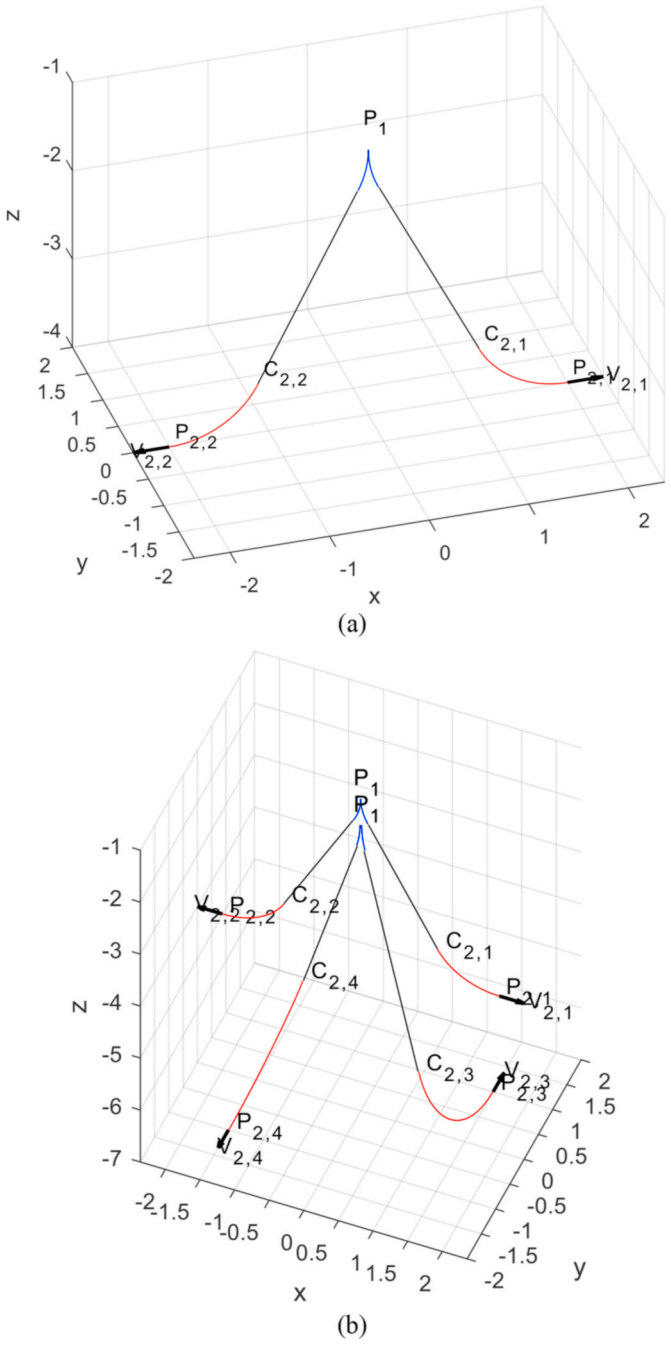

Fig. 6. Optimal drilling site and well trajectories for case 1.2.

$[200, 2100]$ with the resolution of 50 is shown in Fig. 13. The blank area indicates that if the drilling site is located there, then there is at least one completion interval that can't be reached. The data mark indicates the optimal drilling site of the lowest total cost based on the discretized values at the mesh nodes. The exact optimal drilling site location is $(Px_1, Py_1) = (1129.33,\ 606.19)$, and the corresponding optimal cost is 12,518.4. Comparing to the result in Case 2.1, we can see that the 2nd well completion interval almost doesn't affect the optimal drilling site location. The slight effect of the 2nd well completion interval on the cost distribution can be seen from the data marks in Figs. 9 and 13.

4.2.4. Case 2.4

If the maximum allowed turning rate/dogleg severity is increased to 4°/30 m, i.e. minimum allowed turning rate radius is $r_{min} = 429.7$m. The optimal drilling site and well trajectories for the 4 well completion intervals in Table 3 is shown in Fig. 14. The optimal cost distribution of a drilling site where $Px_1 \in [400, 3200]$, $Py_1 \in [200, 2100]$ with the resolution of 50 is shown in Fig. 15. Where we can see there is no more blank area in Fig. 15 compared to Fig. 5. The data mark indicates the optimal drilling site of the lowest total cost based on the discretized values at the mesh nodes. The exact optimal drilling site location is $(Px_1, Py_1) = (1302.38,\ 697.97)$, and the corresponding optimal cost is 20,048.1.

5. Further discussion

1. When there is a turning around in the trajectory, such as the 2nd trajectory in Case 2.2 and we want to avoid such a risk, we can do the following:
   a. Firstly, we can add one more nonlinear constraint Equation (24) into our model Equation (4). Fig. 16 and Fig. 17 show the result of

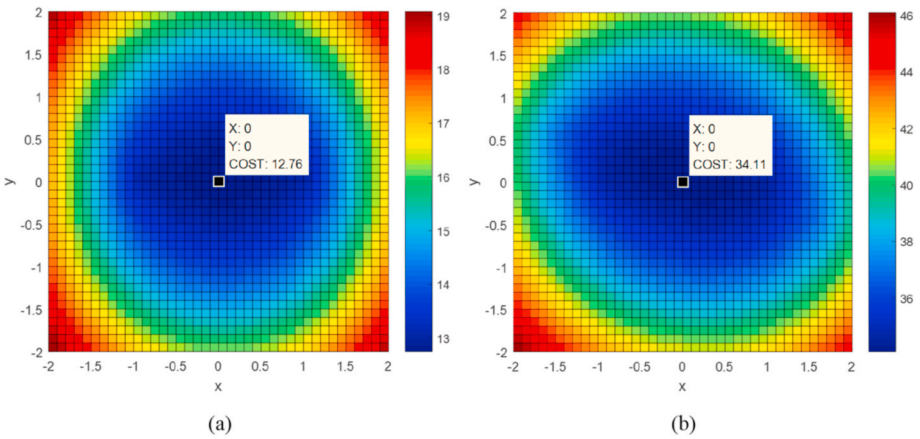

Fig. 7. Optimal cost distribution for case 1.2.

Table 3
Completion intervals in case 2.

Interval No.	Start Point $P_{2,i}$ of Interval	End Point of Interval	Direction Vector $V_{2,i}$
1	(410.90, 209.89, −3850.27)	(413.54, 211.37, −3879.12)	(2.64, 1.48, −28.85)
2	(3011.47, 2098.01, −4368.09)	(2995.05, 2087.54, −4376.20)	(-16.42, −10.47, −8.11)
3	(1784.37, 763.80, −4179.39)	(1789.20, 767.85, −4207.38)	(4.83, 4.05, −27.99)
4	(1475.43, 789.75, −2066.32)	(1482.84, 793.68, −2071.76)	(7.41, 3.93, −5.44)

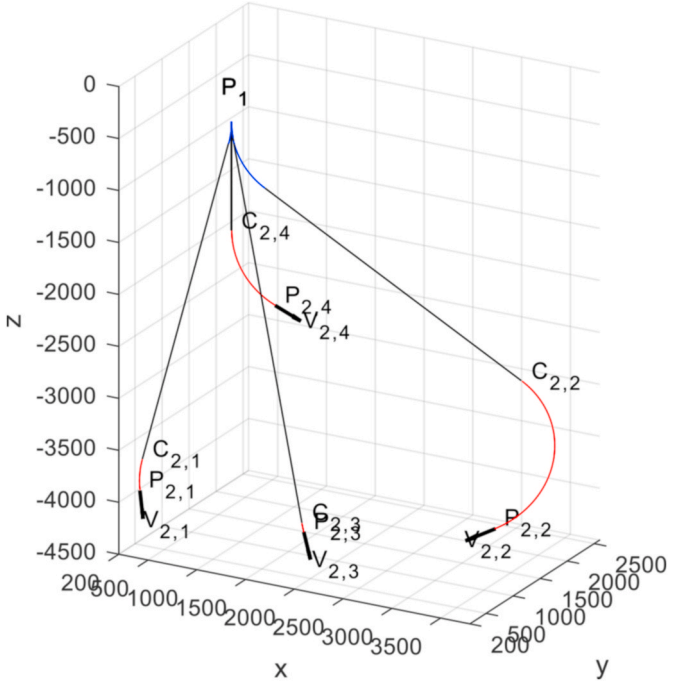

Fig. 8. Optimal drilling site and well trajectories for case 2.1.

Case 2.2 with Equation (24) added as a constraint. Equation (24) limits the turning angle between the straight section and the second curved section to be no larger than 90°. The optimal drilling site location is $(Px_1, Py_1) = (2570.53,\ 1504.94)$, and the corresponding optimal cost is 21,011.91.

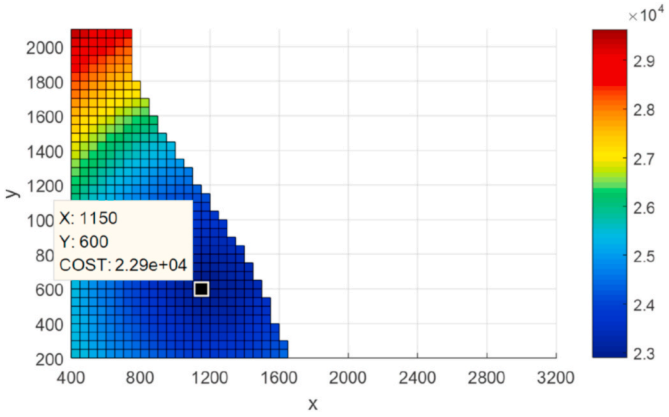

Fig. 9. Optimal cost distribution for case 2.1.

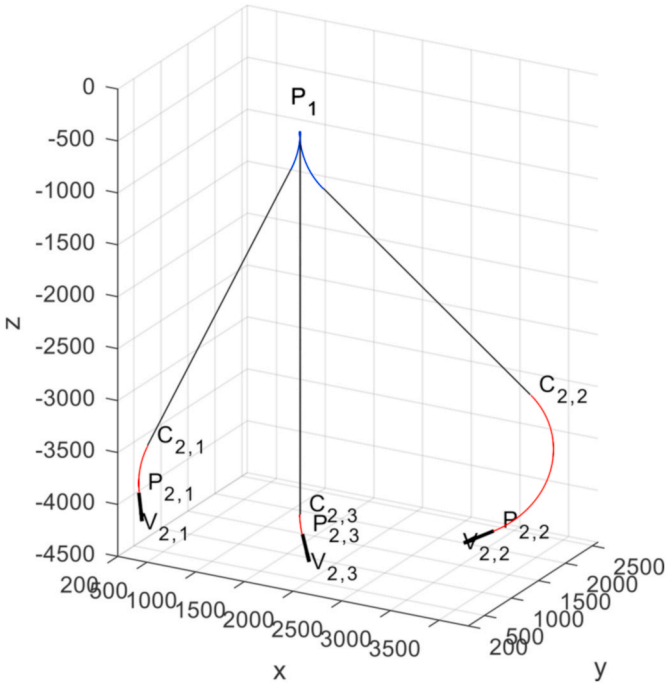

Fig. 10. Optimal drilling site and well trajectories for case 2.2.

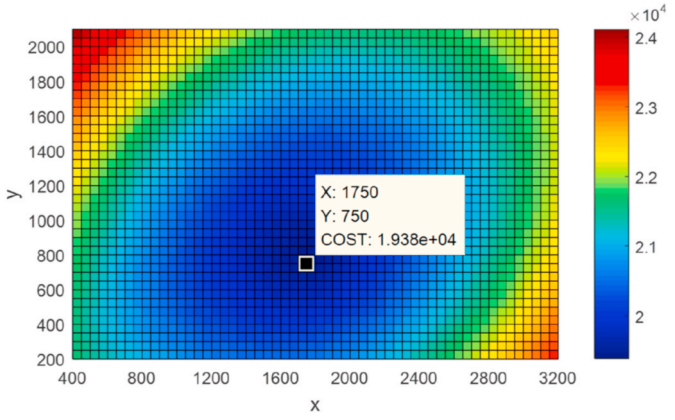

Fig. 11. Optimal cost distribution for case 2.2.

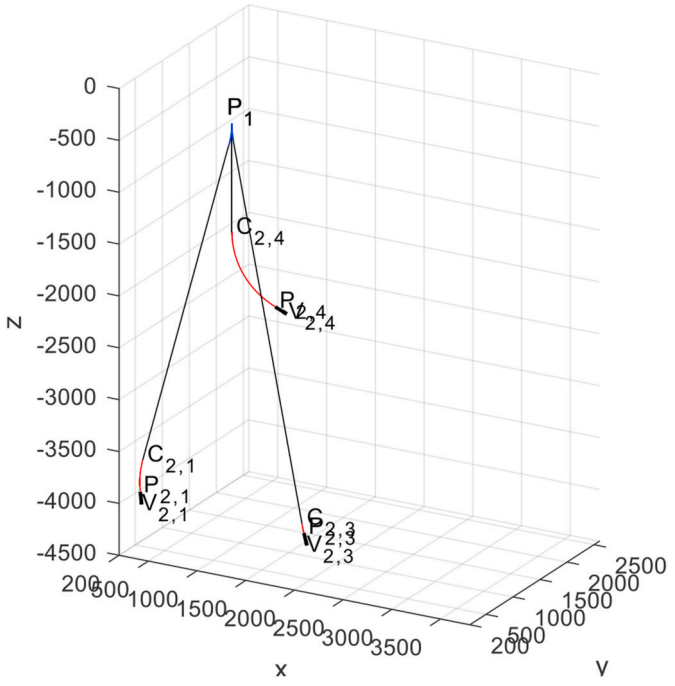

Fig. 12. Optimal drilling site and well trajectories for case 2.3.

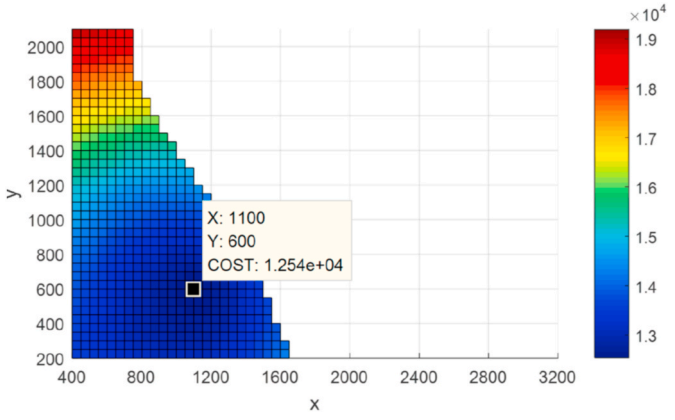

Fig. 13. Optimal cost distribution for case 2.3.

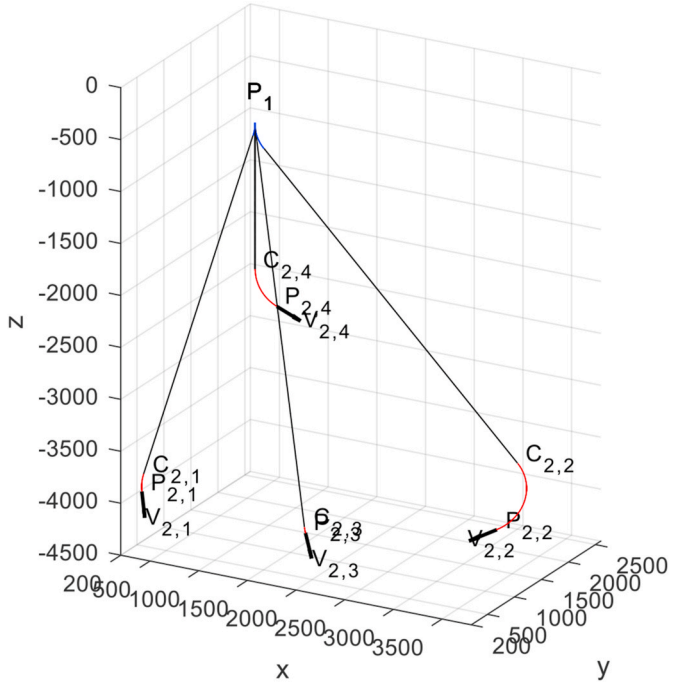

Fig. 14. Optimal drilling site and well trajectories for case 2.4.

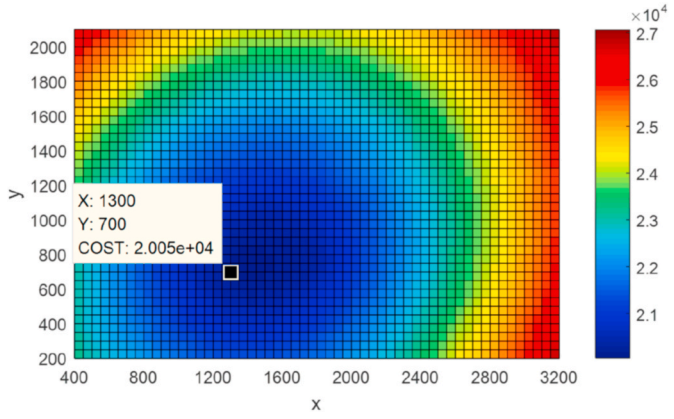

Fig. 15. Optimal cost distribution for case 2.4.

$$\gamma_2 = \arccos\left(\frac{V_2 \cdot T}{\|V_2\| \cdot \|T\|}\right) \le \frac{\pi}{2} \quad \Leftrightarrow \quad T \cdot V_2 \ge 0 \tag{24}$$

b. If the result from step a. is not favorable, then discuss with the geological engineers and reservoir engineers to check if it is possible to modify the completion interval so that the turning around doesn't happen.

c. If modification is also impossible, we should consider two drilling sites for the given intervals. Then the problem will include another challenge problem of finding the best combination of intervals for the drilling sites, which is beyond our study here. Of course, for a small-scale problem, a compromised solution can be that we separate the unwanted interval for a satellite well. And then compare the total cost with the result from step a. As for the challenging "*k*-sites-*n*-wells" problem, kindly refer to our following two papers in the series where we provide an unparalleled efficient method.

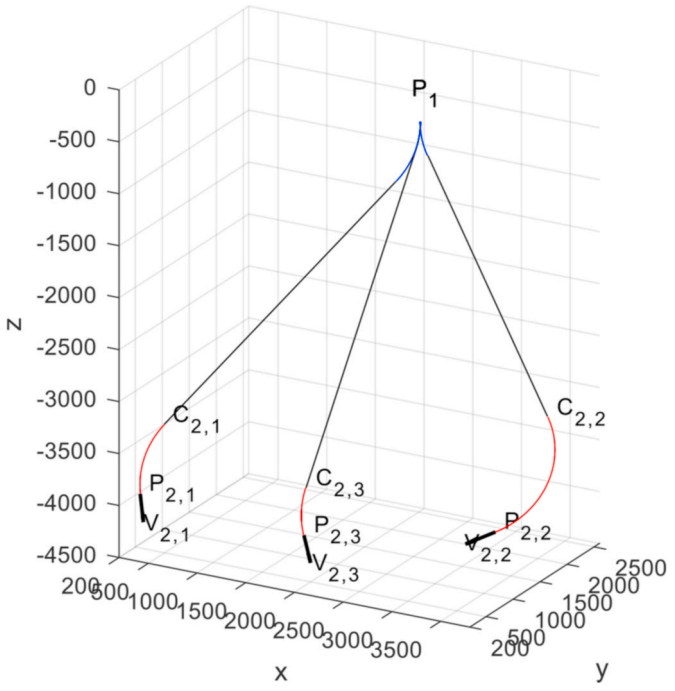

Fig. 16. Optimal drilling site and well trajectories for case 2.2 with turning angle.$\leq 90^{\circ}$

2. We can also easily include the constraint for the drilling site location. For example, if the well location has a limit $Py_1 \leq 1300$ along with the nonlinear constraint Equation (24), we will get the optimal drilling site location at $(Px_1, Py_1) = (2704.44,\ 1300.00)$ with the cost of 21,100.20.
3. We can also include the formation information into the cost function. But the original Dubins curve trajectory no longer guarantees to be the optimal. In order to get the accurate optimized result, we will firstly need to discretize the formation according to the heterogeneity, then optimize all the intermediate nodes between the kickoff point and the well completion interval point. This process is of course much more complicated, but the optimization idea of using the Dubins curve and gradient descent method remains the same. This is a good start point for our future work to make drilling cost estimation more accurate.
4. If we want to find the exact locations of all wellheads $D_i : (Px_{1,i}, Py_{1,i}, 0)$ in one drilling site $D_0 : (Px_1, Py_1, 0)$, we can continue to do a similar optimization process with the all wellheads' locations D_i in the vicinity of the optimized drilling site D_0. Of course, there can be various definition of vicinity, here gives a simple case where D_i are in the radius of Q centered at D_0:

$$\begin{aligned} Obj.\quad & \min_{D_i:(Px_1,Py_1)_i} \sum_{i=1}^{k} COST(P_1, V_1, P_2, V_2, r)_i \\ & = \min_{D_i:(Px_1,Py_1)_i} \sum_{i=1}^{k} [cstC(Lc)_i + cstS(Ls, \theta)_i] \\ s.t.\quad & r_i \geq r_{\min} \\ & Lc_i, Ls_i, \theta_i \in DubinsCurve \\ & Pz_{1,i} = Z_i \\ & \|D_i - D_0\|_2 \leq Q \end{aligned} \tag{25}$$

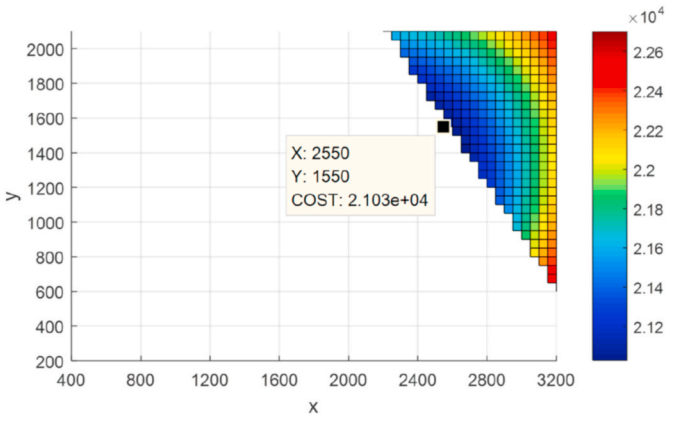

Fig. 17. Optimal cost distribution for case 2.2 with turning angle.$\leq 90^{\circ}$

5. At last, we can also combine this optimization process with the seabed facility layout to obtain the overall optimized subsea field development plan. Of course, we should firstly solve the combinatorial problem just discussed in 1.c.

6. Conclusion

We introduced the concept of Dubins curve for well trajectory planning. Based on the CSC family of 2D Dubins curve, we have proposed an efficient generic 3D well trajectory optimization method which can be a good way to handle the "1-site-*n*-wells" problem. It provides a tool for drilling cost estimation at the early phase of the field development. What is more, our method has very good potential to be more accurate and to be embedded into a systematical method for the overall field layout optimization in more complex scenarios.

Author statement

Haoge Liu: Conceptualization, Methodology, Software, Validation, Formal analysis, Investigation, Data curation, Writing – original draft preparation, Writing- Reviewing and Editing, Visualization. **Tor Berge Gjersvik:** Conceptualization, Validation, Resources, Writing- Reviewing and Editing, Supervision, Project administration, Funding acquisition. **Audun Faanes:** Conceptualization, Validation, Resources, Supervision, Writing- Reviewing and Editing.

Declaration of competing interest

The authors declare that they have no known competing financial interests or personal relationships that could have appeared to influence the work reported in this paper.

Acknowledgement

This work was carried out as a part of SUBPRO(NTNU-SUBPRO), a Research-based Innovation Centre within Subsea Production and Processing. We gratefully acknowledge the project support from SUBPRO (grant number 237893), which is financed by the Research Council of Norway, major industry partners and NTNU.

Appendix I. List of Symbols

k: number of completion intervals;
$P_{1,i}$: kickoff point for the $i-$ thwell, 3D coordination is $(Px_1, Py_1, Pz_{1,i})$;
$V_{1,i}$: drilling direction vector of the $i-$ thwell, in this study all $V_{1,i}$ is $(0, 0, -1)$;
$P_{2,i}$: start point of the $i-$ thwell completion interval, 3D coordination is $(Px_{2,i}, Py_{2,i}, Pz_{2,i})$;
$V_{2,i}$: drilling direction vector of the $i-$ thwell completion interval, 3D coordination is $(Vx_{2,i}, Vy_{2,i}, Vz_{2,i})$
Z_i: highest kickoff point for $i-$ thwell.
κ: max allowed turning rate/dogleg severity, $^\circ$/100m.
$r_{\min}$: minimum allowed turning radius, m.
D: optimal drilling site, 3D coordination is $(Px_1, Py_1, 0)$
Lc: length of the non-straight/circular section;
Ls: length of the straight section;
θ: deviation angle of the straight section;
$cstC(Lc)$: cost function of the non-straight section;
$cstS(Ls, \theta)$: cost function of the straight section;
$COST(P_1, V_1, P_2, V_2, r)_i$: cost function of the $i-$ thwell.
T: straight section vector in the Dubins curve

Note:

1. For the subscription i denoting the parameters of the $i-$ th well, it maybe ommited such as $(Px_1, Py_1, Pz_{1,i})$ when all wells share the same value or when we are just focusing on one specific well such as Equation (1). The subscription i may also be merged outside the parenthesis such as Equation (4).
2. Some symbols related with Dubins curve are not listed here as they are not used other than Section 3.2.

References

Amorim Jr., D.S., Santos, O.L.A., Azevedo, R.C.d., 2019. A statistical solution for cost estimation in oil well drilling. REM Int. Eng. J. 72, 675–683. https://doi.org/10.1590/0370-44672018720183.

Chitsaz, H., Lavalle, S.M., 2008. Time-optimal paths for a Dubins airplane. In: 2007 46th IEEE Conference on Decision and Control. IEEE. https://doi.org/10.1109/CDC.2007.4434966.

Dubins, L.E., 1957. On curves of minimal length with a constraint on average curvature, and with prescribed initial and terminal positions and tangents. Am. J. Math. 79, 497–516. https://doi.org/10.2307/2372560.

Hota, S., Ghose, D., 2010. Optimal geometrical path in 3D with curvature constraint. In: 2010 IEEE/RSJ International Conference on Intelligent Robots and Systems. IEEE. https://doi.org/10.1109/IROS.2010.5653663.

Ilyasov, R.R., Svechnikov, L.A., Karimov, M.R., Kravets, M.Z., Solodov, A.N., Porolo, I.O., 2014. Automation of optimal well trajectory calculations. In: SPE Russian Oil and Gas Exploration & Production Technical Conference and Exhibition, Moscow, Russia. SPE. https://doi.org/10.2118/171326-MS.

Johnson, H.H., 1974. An application of the maximum principle to the geometry of plane curves. Proc. Am. Math. Soc. 44, 432–435. https://doi.org/10.2307/2040451.

Liu, Z., Samuel, R., 2014. Wellbore trajectory control using minimum well profile energy criterion for drilling automation. In: 2014 SPE Annual Technical Conference and Exhibition, Amsterdam, The Netherlands. SPE. https://doi.org/10.2118/170861-MS.

McMillian, William H., 1981. Planning the directional well - A calculation method. J. Petrol. Technol. 33 (06), 952–962. https://doi.org/10.2118/8337-PA.

Mittal, M., Samuel, R., 2016. 3D downhole drilling automation based on minimum well profile energy. In: 2016 SPE Annual Technical Conference and Exhibition, Dubai, UAE. SPE. https://doi.org/10.2118/181381-MS.

NTNU-SUBPRO. Available: https://www.ntnu.edu/subpro/.

Owen, M., Beard, R.W., McLain, T.W., 2015. Implementing Dubins airplane paths on fixed-wing UAVs*. In: Valavanis, K.P., Vachtsevanos, G.J. (Eds.), Handbook of Unmanned Aerial Vehicles. Springer Netherlands, Dordrecht, pp. 1677–1701. https://doi.org/10.1007/978-90-481-9707-1_120.

Patsko, Valerii S., Turova, Varvara L., 2009. From Dubins' car to Reeds and Shepp's mobile robot. Comput. Visual. Sci. 12, 345–364. https://doi.org/10.1007/s00791-008-0109-x.

Pharpatara, P., Hérissé, B., Bestaoui, Y., 2015. 3D-shortest paths for a hypersonic glider in a heterogeneous environment. IFAC-PapersOnLine 48, 186–191. https://doi.org/10.1016/j.ifacol.2015.08.081.

Samuel, R., 2010. A new well-path design using clothoid spiral (curvature bridging) for ultra-extended-reach drilling. SPE Drill. Complet. 25, 363–371. https://doi.org/10.2118/119459-PA.

Sawaryn, S.J., Thorogood, J.L., 2005. A compendium of directional calculations based on the minimum curvature method. SPE Drill. Complet. 20, 24–36. https://doi.org/10.2118/84246-PA.

Shengzong, J., Xilu, W., Limin, C., Kunfang, L., 1999. A new method for designing 3D trajectory in sidetracking horizontal wells under multi-constraints. In: 1999 SPE Asia Pacific Improved Oil Recovery Conference, Kuala Lumpur, Malaysia. SPE. https://doi.org/10.2118/57282-MS.

Skaugset, Kjetil, 2015. Subsea Cost Reduction. April 24th,. OG21. https://www.og21.no/contentassets/f826df43db324d79b148a14cfcf912c4/tta4-subsea-cost-report.pdf .

Sussmann, H.J., 1995. Shortest 3-dimensional paths with a prescribed curvature bound. In: Proceedings of 1995 34th IEEE Conference on Decision and Control, vol. 4. IEEE, pp. 3306–3312. https://doi.org/10.1109/CDC.1995.478997.

Taylor, H.L., Mason, M.C., 1972. A systematic approach to well surveying calculations. Soc. Petrol. Eng. J. 12, 474–488. https://doi.org/10.2118/3362-PA.

Wang, Y.H., 2018. 3D Dubins Curves for Multi-Vehicle Path Planning. MSc Thesis. Electrical and Computer Engineering, Missouri University of Science and Technology. https://scholarsmine.mst.edu/masters_theses/7839.

Wang, Z., Gao, D., Yang, J., 2019. Design and calculation of complex directional-well trajectories on the basis of the minimum-curvature method. SPE Drill. Complet. 34 (02), 173–188. https://doi.org/10.2118/194511-PA.

Yi, P., Samuel, R., 2015. Downhole automation using spline, catenary, and clothoid curves based on minimum wellpath energy. In: 2015 SPE/IADC Drilling Conference and Exhibition, London, England, UK. SPE. https://doi.org/10.2118/173096-MS.

Zaremba, W.A., 1973. Directional survey by the circular arc method. Soc. Petrol. Eng. J. 13 (01), 5–11. https://doi.org/10.2118/3664-PA.